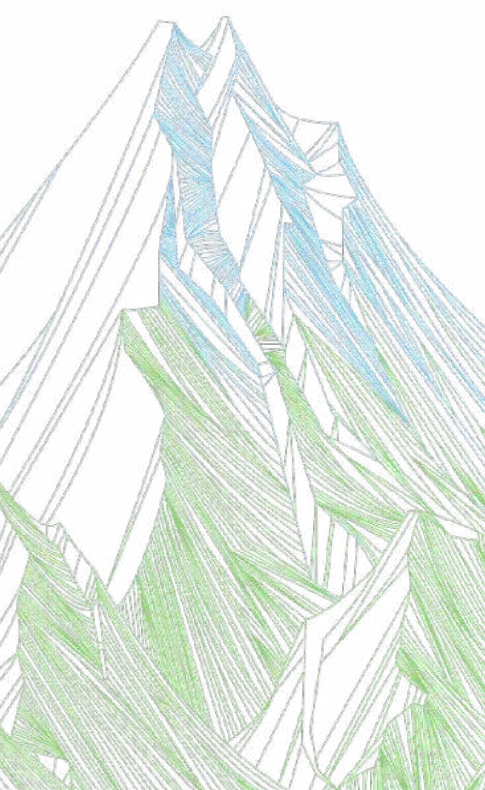




X-RISK-CC pilot areas (top) and the pilot area of the Eleanor storm – Arly river catchment (bottom)

WINTER STORM ELEANOR IN THE SAVOY ALPS – ARLY RIVER CATCHMENT

France

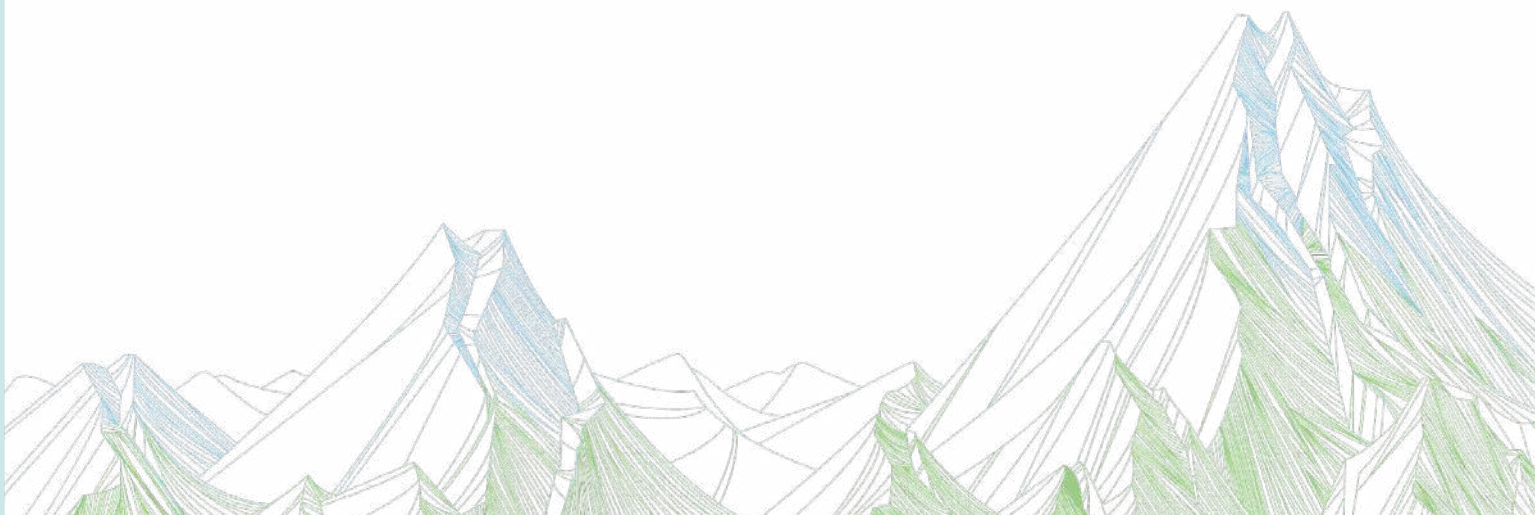


Pilot report prepared by Slovenian Environment Agency, EURAC Research and GeoSphere Austria with the support of the X-RISK-CC partnership

TABLE OF CONTENTS



KEY MESSAGES	3
PAST EXTREME EVENTS IN FOCUS	4
DEFINITION OF METEOROLOGICAL EXTREMES	5
TYPICAL SYNOPTIC SITUATION LEADING TO THE EXTREME EVENT	7
CHARACTERISTICS OF EXTREME EVENTS IN THE PAST	9
WHAT TO EXPECT IN THE FUTURE?	14
METHODOLOGY	16



KEY MESSAGES



- The relevant weather extremes in the catchment area of the Arly river, leading to avalanches, mudflows, rockfalls, landslides, flooding and other damage in the region, are intense 1- to 5-day precipitation events associated with strong winds.
- An example of such events was winter storm Eleanor, which occurred in January 2018. Locally it brought over 130 mm of rain over two days (a rare event for winter in this area with an estimated return period of 30 years) in combination with strong winds reaching 70 km/h and wind gusts up to 115 km/h.
- In the period 1991–2022 there was an increasing trend in 1-day precipitation intensity for spring (5–15 % increase per decade) and a decreasing trend in 1-, 3- and 5- day precipitation intensity in autumn (5–15 % decrease per decade) in the Arly catchment. No trends in precipitation intensity were observed for winter or on an annual level. The frequency of extreme precipitation days in the Arly river catchment shows no significant changes over time, regardless of the season or considered accumulation period.
- Significant changes in the intensity and frequency of wind speed extremes were observed for half of the stations in the Arly river catchment in the period 1991–2022. Extreme wind speed and the number of extreme wind days decreased in Albertville in winter, and in Bourg St. Maurice in winter, summer and on an annual level. The slightly higher Col-des-Saisies station shows an increase in extreme wind days in summer (+1.5 days per decade) and wind speed intensity (+1.5 m/s per decade).
- In the future, precipitation extremes will be more frequent and more intense. The climate projections for the Arly river catchment show that the annual and winter maximum 1- to 5-day precipitation will be up to 10 % higher, while the summer maximum multi-day precipitation will decrease. On an annual level, the number of days with extreme 1-day precipitation will increase by 25 % and the number of days with extreme 2- to 3-day precipitation will increase by 20 %. Seasonally, the highest increase in the frequency of precipitation extremes is expected in winter (up to 40 % for 1-day and 20 % for 2- to 3-day precipitation), while the changes in frequency are lower in spring and autumn (less than 20 %).
- The number of days with extreme daily mean wind speed is likely to increase by about 10 % on an annual level and in winter under a global warming level of 4 °C (GWL4). Similarly, the maxima of daily mean wind speed are also likely to increase slightly under GWL4 on an annual level and in winter (by around 3 %).



PAST EXTREME EVENTS IN FOCUS



WINTER STORM ELEANOR IN JANUARY 2018

Storm Eleanor was an extratropical cyclone that hit several European countries (from Ireland to Austria) between 2nd and 5th January 2018. In France, with wind speeds of over 130 km/h, intense precipitation and temperature rise leading to rain-on-snow episodes, Eleanor emerged in a context already weakened by other storms that had occurred previously and with

water-saturated soils. In the case study area of the Arly river catchment in the Savoy Alps, the event led to a sharp increase in instability phenomena: avalanches, mudflows, rockfall, landslides and torrential flooding (Stoffel and Corona, 2018; Barthelon, 2018). The storm caused extensive damage and traffic disruption in many municipalities. Eleanor was estimated to be the sixth strongest storm in Europe since 1995 with an estimated return period at around 20 years in the current climate and an estimated economic impact of 700 million euros (Vautard et al., 2019).

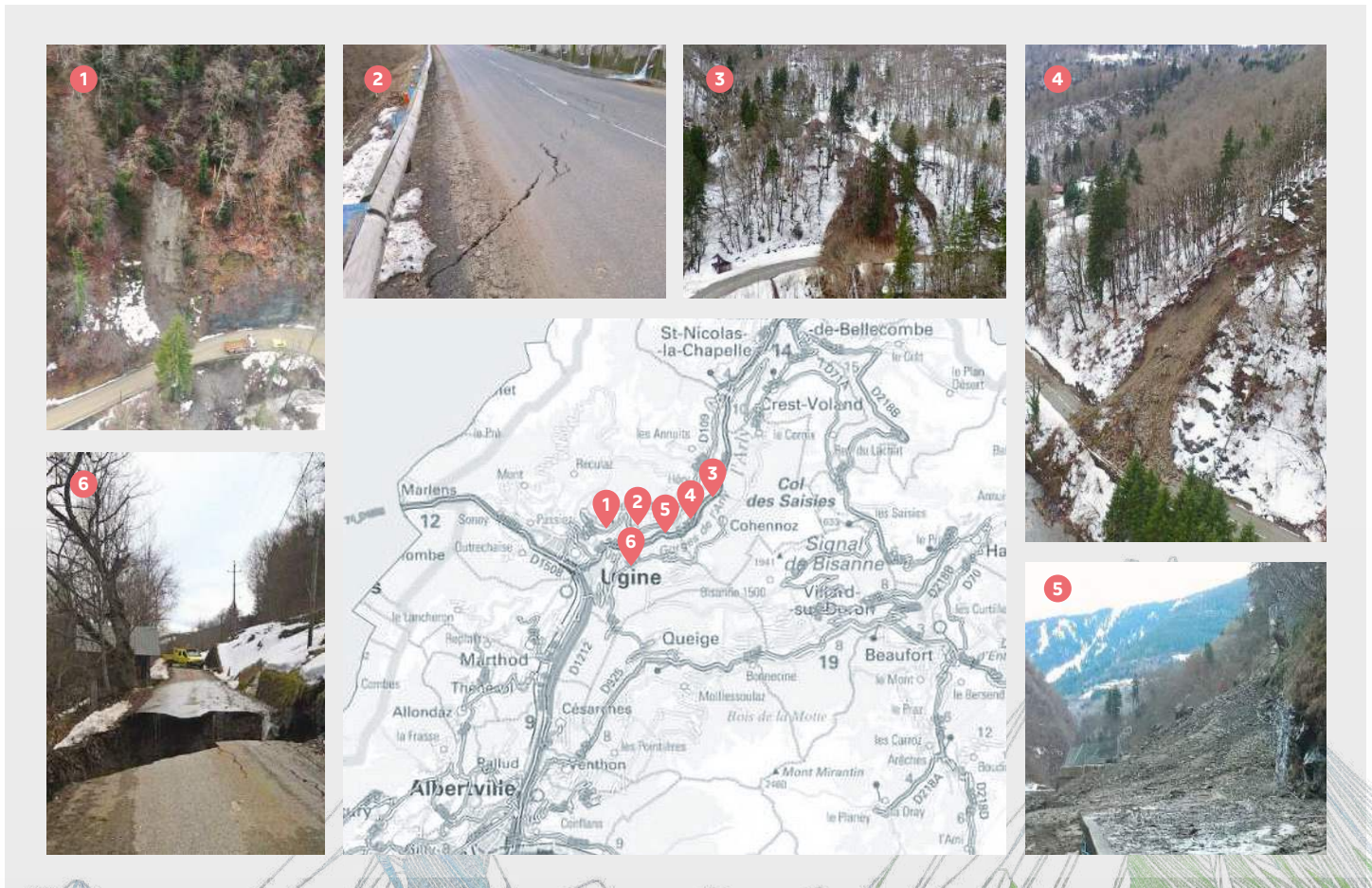


FIGURE 1: Examples of hazards that affected the area between Ugine and Albertville following the events of January 2018. Source: Département de Savoie (Lescurier, 2018).

DEFINITION OF METEOROLOGICAL EXTREMES



EXTREME PRECIPITATION

Rx1d, Rx2d, Rx3d, Rx5d:

annual and seasonal precipitation maxima over 1, 2, 3 and 5 days

R97pN:

annual and seasonal number of days with daily to multi-daily precipitation exceeding the 97th percentile of the reference period 1991–2020 (percentile calculated from wet days with 1 mm or more precipitation)

EXTREME WIND SPEED

WSx1d*:

annual and seasonal maxima of the daily maximum wind speed, with the daily maximum wind speed defined as the maximum of 10-min averages

WS97pN_1d*:

annual and seasonal number of days with daily maximum wind speed exceeding the 97th percentile of the reference period 1991–2020

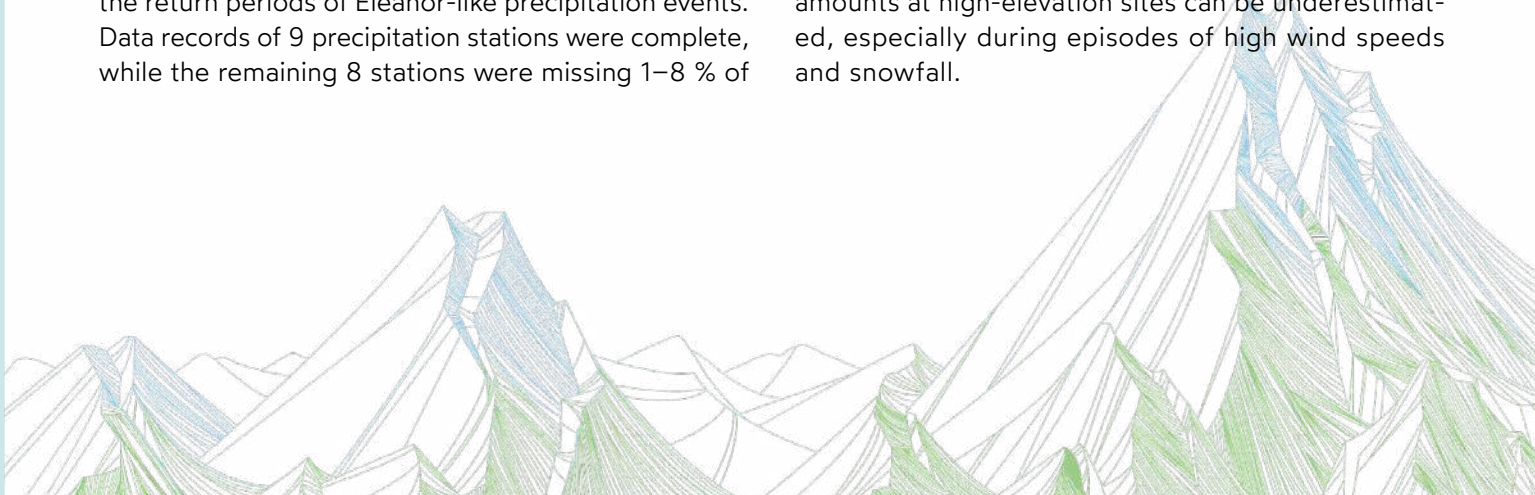
*daily mean wind speed used for future projections



DATA

For the Eleanor case study area – the Arly river catchment – observations of daily precipitation at 17 stations and daily maximum wind speed at 4 stations were used to analyse extreme daily to multi-daily precipitation events and extreme daily wind speeds in the period from 1990 to 2022 (**FIGURE 2**), while 9 of these stations with longer data records (1950–2022) were used to assess the return periods of Eleanor-like precipitation events. Data records of 9 precipitation stations were complete, while the remaining 8 stations were missing 1–8 % of

the data. For the maximum daily wind speed, 2–19 % of the data are missing. All datasets have undergone climatological control by Météo-France but were not homogenised, therefore the time series can contain inhomogeneities. This should be taken into account when interpreting the results. It is also important to consider that the observations can still be affected by uncertainties, especially in areas characterized by complex orography. In particular, precipitation amounts at high-elevation sites can be underestimated, especially during episodes of high wind speeds and snowfall.



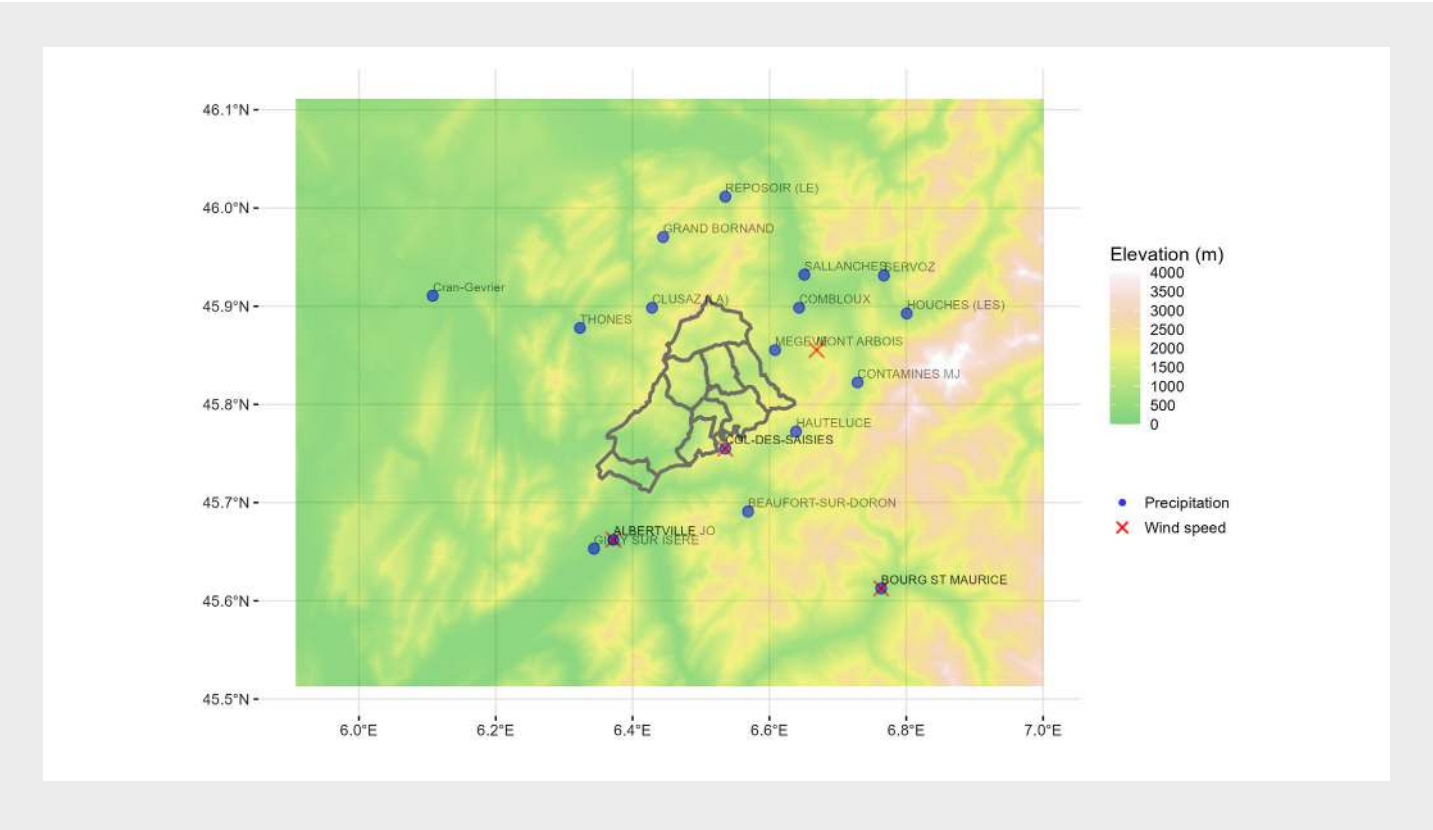


FIGURE 2: Precipitation and wind speed stations in the wider area of Arly river catchment. The blue dots indicate 17 precipitation stations and red crosses 4 wind speed stations. The boundary of the upper Arly river catchment (from Megève to Ugine) is marked with a grey line.

The analysis of future changes in the frequency and intensity of extreme precipitation and wind speed is based on daily precipitation and wind speed projections from the bias-adjusted EURO-CORDEX climate simulations DRIAS-20 (Drias, data Météo-France, CERFACS, IPSL, 2024), implemented by Météo-France using the SAFRAN observational database, with a resolution of 8 km (**TABLE 1**). Since projections of maximum daily wind speed were not available from DRIAS-2020 simulation ensemble over France and the wind speed observation data in the Arly catchment area were not suitable for bias

adjustment, future changes in wind speed over the Arly catchment were estimated from daily mean wind speed.

It is important to note that station observations and model simulations are not directly comparable, even after the bias-adjustment procedure, which increases the overall accuracy of the model fields but does not increase the spatial scales resolved. The coarser spatial resolution of the model simulations therefore limits the representation of features at the local scale, especially in orographically-complex regions.

TABLE 1: List of bias-adjusted EURO-CORDEX model simulations DRIAS-20 used for evaluation of projected changes in extreme precipitation and wind speed in Eleanor pilot area (Arly river catchment).

	Global Climate Model	Regional Climate Model (Institute)
1	MPI-ESM-LR	CCLM4-8-17 (CLMcom)
2	EC-EARTH	RCA4 (SMHI)
3	EC-EARTH	RACMO22E (KNMI)
4	CNRM-CM5	RACMO22E (KNMI)
5	CNRM-CM5	ALADIN63 (CNRM)
6	MPI-ESM-LR	REMO2009 (MPI)

TYPICAL SYNOPTIC SITUATION LEADING TO THE EXTREME EVENT

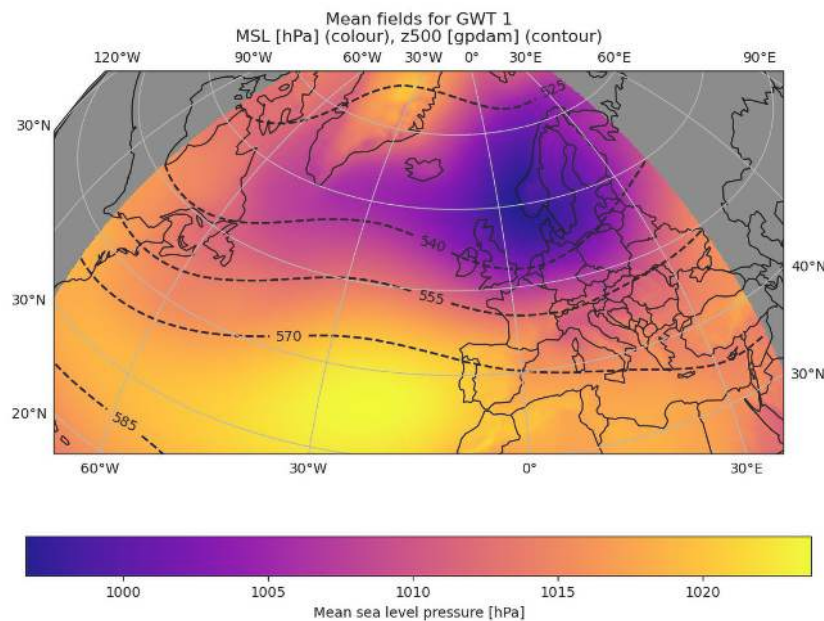


FIGURE 3: Prevailing GWT for Eleanor: GWT 1. Mean sea level pressure is shown in colours, 500 hPa geopotential as contours.

The prevailing circulation type for Eleanor is GWT 1 ('Gross-Wetter-Type'; a circulation type classification), which can be seen in **FIGURE 3**. The large-scale circulation is governed by a low-pressure system between the British Isles and Scandinavia. The corresponding through reaches into Central Europe, which causes westerlies and precipitation in the Western Alps. During the event, the GWT was stationary, which in the case of Eleanor means continuous precipitation. Specifically, **FIGURE 4** shows the daily mean fields from ERA5 data over the event duration. It is clearly visible that westerlies prevail over the duration of the event. Furthermore, toward the end of the event, the low-pressure system and the large-scale trough have moved past Central Europe and the Western Alps were being affected by a ridge, bringing warmer air. This caused the unusual temperature increase immediately after the event. To study

potential changes, we used 3-day consecutive GWT 1 as indicator for similar such events. **FIGURE 5** shows the 3-day consecutive GWT 1 counts for each season over the past 70 years. No significant trend is visible, indicating that the dynamic component (i.e. circulation) of such events does not change substantially.

Note that GWTs only capture the large-scale circulation of the weather situation and serve as preconditioning for extreme weather events. However, the existence of a specific GWT class alone does not entail extreme weather events all the time. There are more fine-grained details and thermodynamic components that also play a role in any specific weather situations. Nevertheless, the GWT analysis allows to estimate large-scale circulation changes and therefore changes to the preconditioning relevant for extreme weather events.

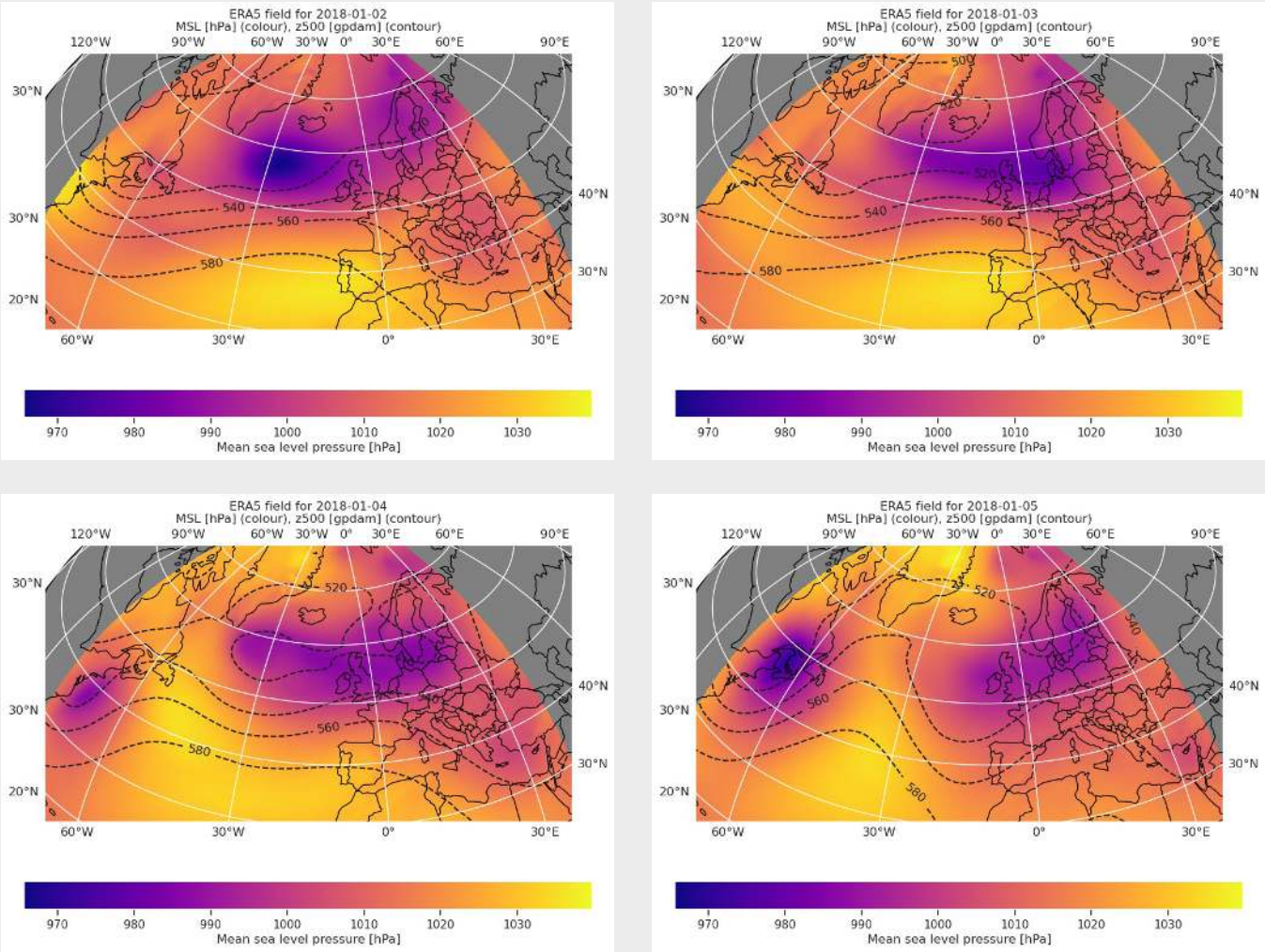


FIGURE 4: Mean sea level pressure and geopotential height in 500 hPa for Eleanor based on ERA5 reanalysis data. Mean sea level pressure is shown in colours, 500 hPa geopotential as contours.

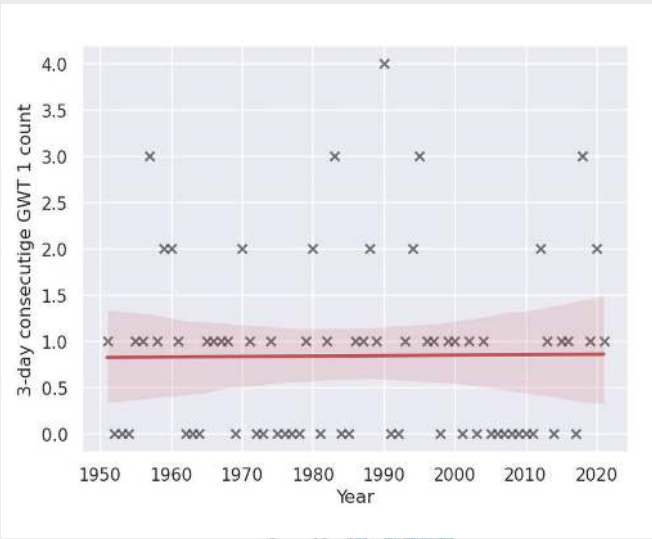


FIGURE 5: 3-day consecutive GWT 1 counts per DJF season (meteorological winter) for each year (December of the previous year was added to the current year). No significant trend can be seen from the historical data. Note that this only depicts the dynamic component, i.e., the circulation, that is associated to that event.

CHARACTERISTICS OF EXTREME EVENTS IN THE PAST



EXTREME PRECIPITATION AND WIND SPEED DURING STORM ELEANOR IN JANUARY 2018

From a meteorological perspective, storm Eleanor was characterised by extreme precipitation and extreme winds. In the pilot area of the Arly river catchment it brought the largest amount of precipitation over a period of 2 days, where a maximum of 132 mm was recorded at the La Clusaz station with an estimated return period of 20 years on an annual scale and 30 years for winter, indicating that such meteorological events occur less frequently in winter (**TABLE 2**). The maximum observed 2-day precipitation accumulations

recorded during the storm ranged from 80 to 130 mm, depending on the station, but none of the observed values during the event reached historical record values (**FIGURE 6**). The return period of maximum 2-day precipitation recorded during storm Eleanor largely depends on precipitation amount and location, ranging from 3 to more than 30 years for winter.

The maximum recorded daily wind speed in the region was 70 km/h at Col de Saisies, a slightly elevated station at 1614 m above sea level, while the maximum instantaneous wind speed (wind gust) reached approximately 115 km/h. Due to the short data records, it was not possible to assess the return periods for extreme winds with a high degree of certainty.

TABLE 2: Observed maximum precipitation and wind speed during storm Eleanor at meteorological stations in the case study area.

Variable	Measured value (station)	Return period
1-day precipitation	75 mm (La Clusaz) 100 mm/24h from hourly data (Cohenoz)*	~ 5 years (annual) ~ 14 years (winter)
2-day precipitation	132 mm (La Clusaz)	~ 20 years (annual) ~ 30 years (winter)
3-day precipitation	138 mm (Hauteluce, La Clusaz)	~ 5–8 years (annual) ~ 6–9 years (winter)
Daily maximum wind speed (10 min averages)	70 km/h (Col des Saisies)	short data record
Maximum wind gust (instantaneous)	115 km/h (Col des Saisies, Mont Arbois) 120 km/h from hourly data (La Giettaz)*	short data record

*information obtained from sub-daily measurements

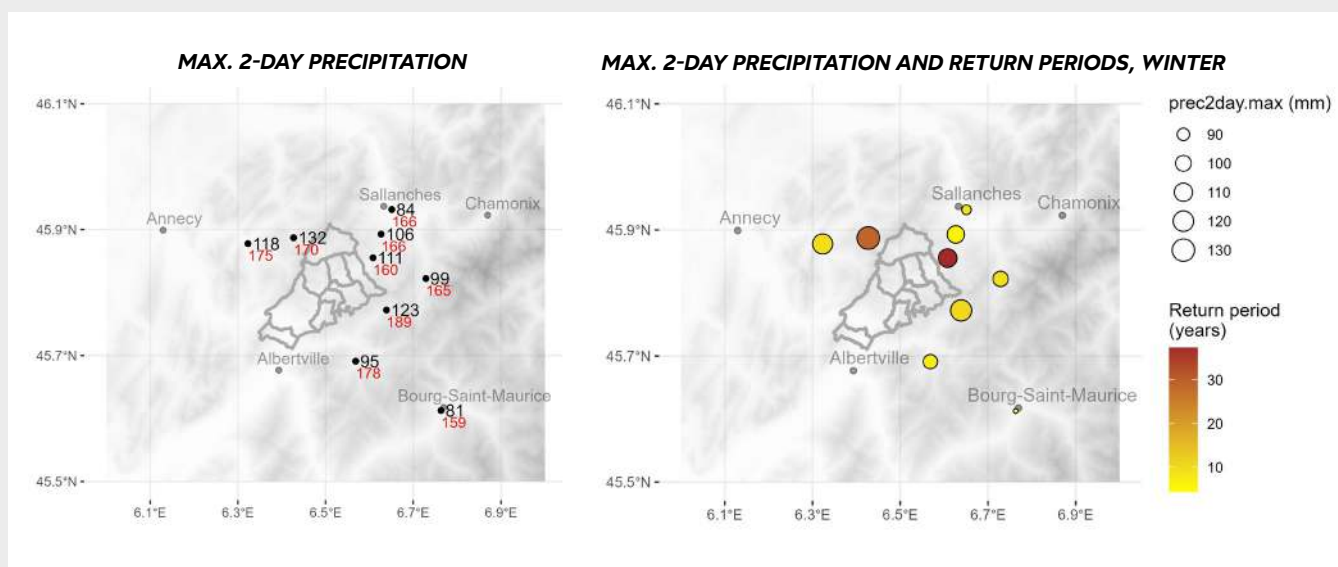


FIGURE 6: Maximum 2-day precipitation during storm Eleanor in 2018, including estimated return periods for winter. On the left, black denotes the measured value while red denotes the record value in the period 1990–2022. On the right, the size of the circles corresponds to the extreme values and the colour of the circles to the estimated return period for winter.

EXTREME PRECIPITATION: TRENDS IN FREQUENCY AND INTENSITY IN THE PERIOD 1990–2022

The frequency of extreme precipitation days in the case study area of the Arly catchment shows no significant changes over time. Linear trends in the number of days above the 97th percentile of the reference period 1991–2020 (considering only wet days with precipitation equal to or above 1 mm) generally show no statistical significance for the considered accumulation periods (1 to 5 days), regardless of the season.

Precipitation intensity, defined as the maximum annual or seasonal value of precipitation accumulation over the period of 1 to 5 days, shows significant changes over time, especially for autumn and spring on a limited number of stations, whereas for winter, the main season of interest, no statistically significant trends are observed. For maximum 1-day precipitation, there is a positive trend at approximately 5 to 15 %/decade for spring and a negative trend at approximately –5 to –15 %/decade for autumn, depending on the station (**FIGURE 7**). For longer accumulation periods, significant trends are observed mainly for autumn, ranging from –5 to –15 %/decade for the maximum 3-day and the maximum 5-day precipitation (**FIGURE 8**).



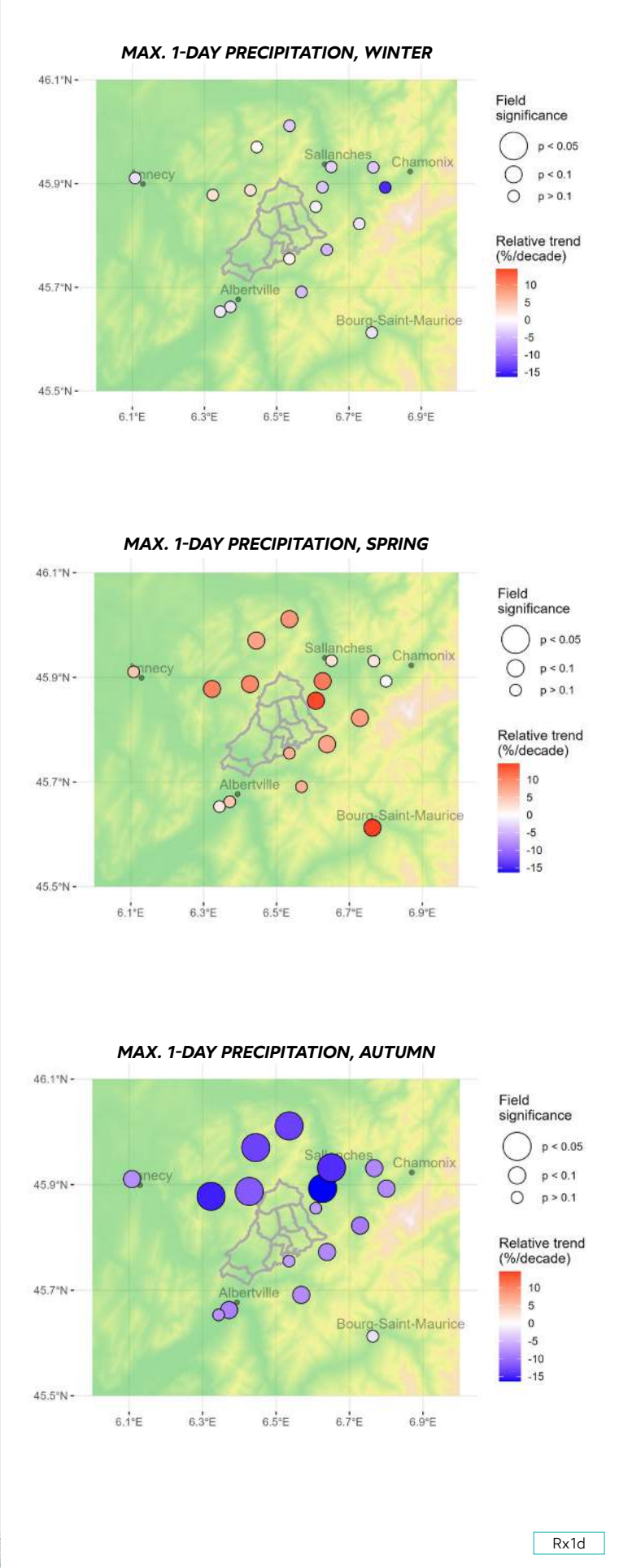


FIGURE 7: Relative trends in maximum 1-day precipitation for winter (top), spring (middle) and autumn (bottom) in the period 1990–2022, including field significance to account for spatial dependence between different stations in the pilot area.

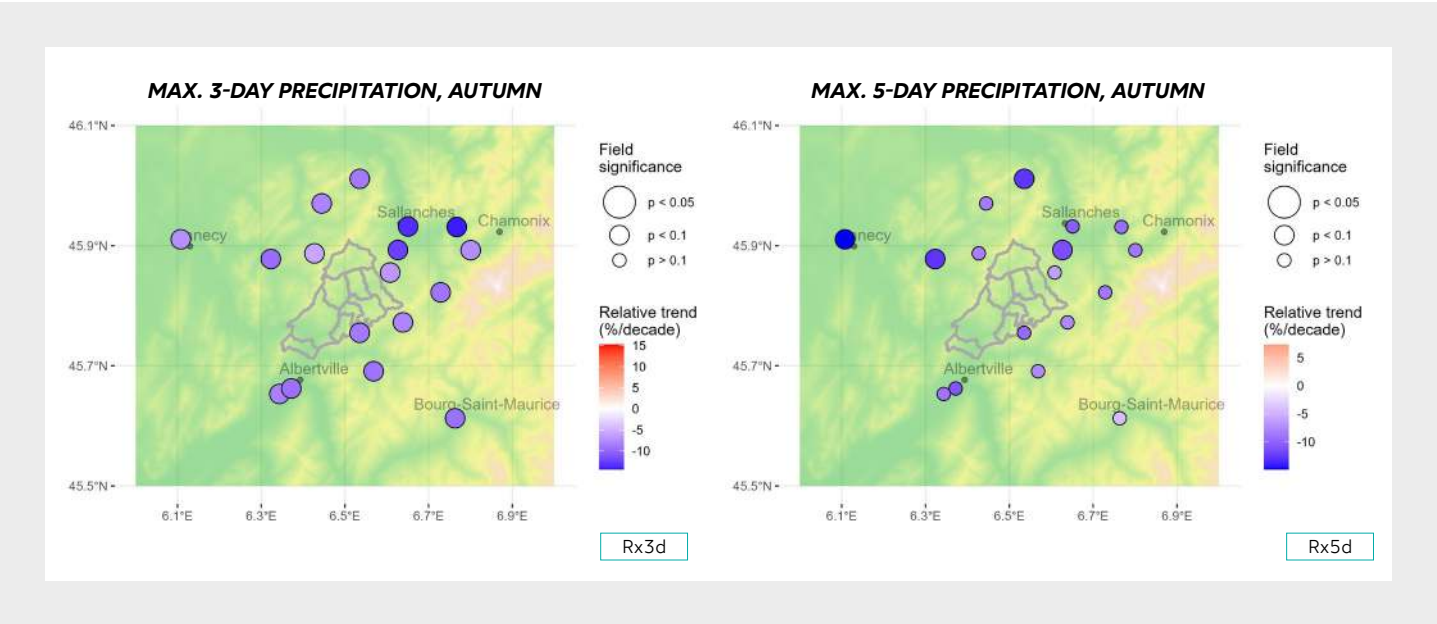


FIGURE 8: Relative trends in maximum 3-day (left) and 5-day (right) precipitation for autumn in the period 1990–2022, including field significance to account for spatial dependence between different stations in the pilot area.

**EXTREME WIND SPEED:
TRENDS IN FREQUENCY AND INTENSITY
IN THE PERIOD 1990–2022**

The frequency of days with extreme wind speed in the past depends on the location and the season. The trend in the number of days on which the wind speed exceeds the 97th percentile of the reference period 1991–2020 is statistically significant for half of the stations in the case study area (**FIGURE 9**). Of the stations in the Arly

catchment area, the Albertville station shows a negative trend of –1 day/decade for winter, while the slightly higher Col-des-Saisies station shows a positive trend of +1.5 days/decade for summer. For the Bourg St. Maurice station in the southeast, a consistent negative trend of –1.5 days/decade can be observed on an annual scale (not shown), –0.8 days/decade for winter and –0.6 days/decade for summer. However, this station is located in a different valley with possibly different characteristics, and therefore may not be fully representative of conditions in the Arly catchment.

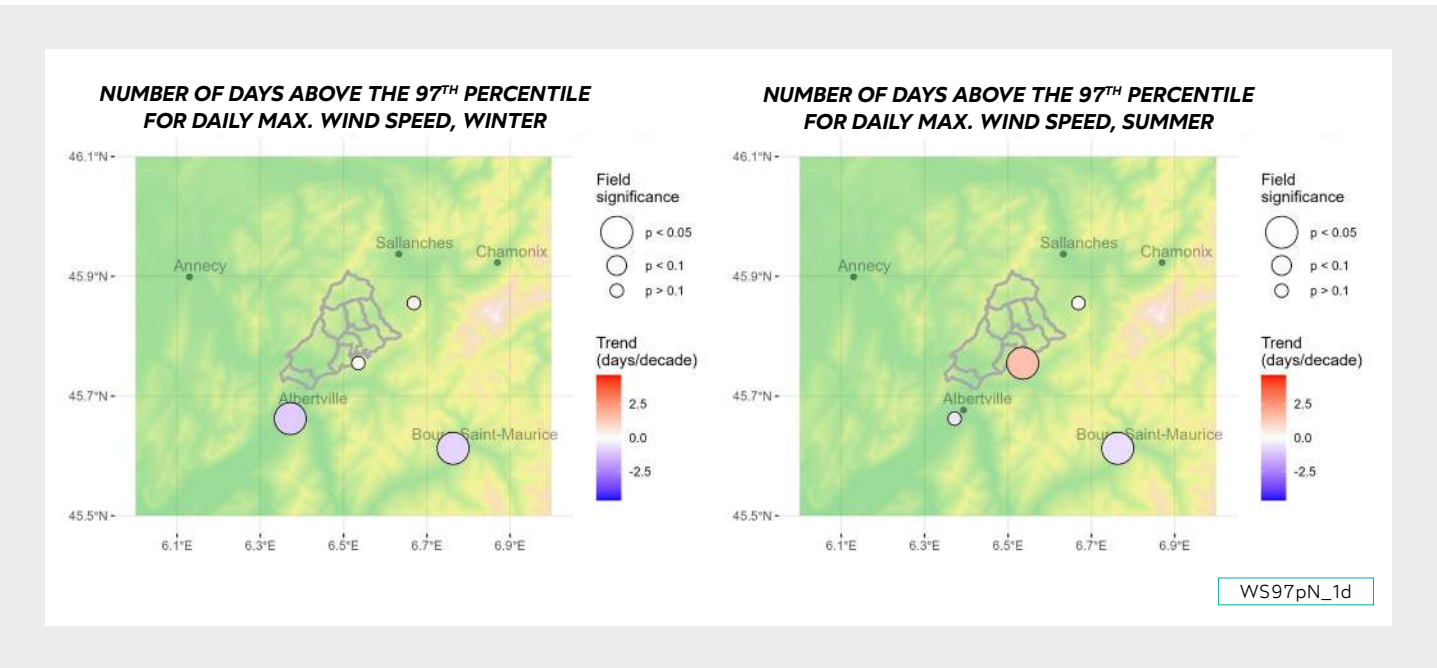


FIGURE 9: Trends in the number of days with maximum daily wind speed above the 97th percentile of the reference period (1991–2020) for winter (left) and summer (right) in the period 1990–2022, including field significance to account for spatial dependence between different stations in the pilot area.

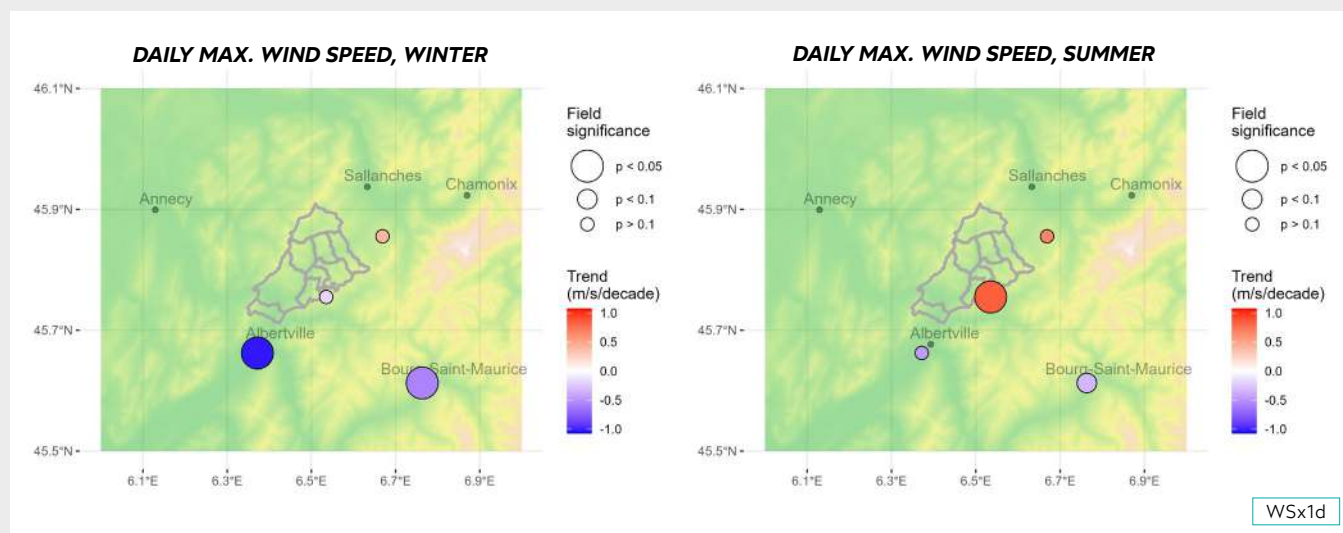


FIGURE 10: Trends in maximum daily wind speed for winter (left) and summer (right) in the period 1990–2022, including field significance to account for spatial dependence between different stations in the pilot area.

The general direction of the trends in maximum daily wind speed intensity aligns with the direction of the trends in the occurrence of days with extreme wind speed. Similar to the number of days above the 97th percentile, we observe a negative trend in maximum intensity for station Albertville in the Arly catchment

of -1 m/s/decade for winter and a positive trend of 1.5 m/s/decade for the slightly higher station Col-des-Saisies in summer (**FIGURE 10**). For the Bourg St. Maurice station, negative trends in wind speed intensity can be observed for all seasons, ranging from -0.3 m/s/decade in summer to -0.9 m/s/decade in winter.



WHAT TO EXPECT IN THE FUTURE?

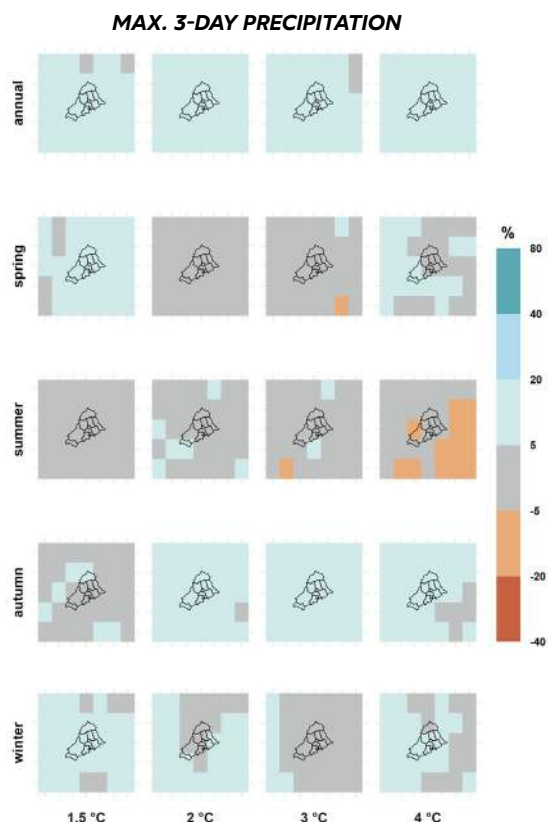


HOW WILL EXTREME PRECIPITATION EVENTS CHANGE?

In the future, the annual and seasonal precipitation amounts over the wider area of the Arly catchment will be slightly higher (up to 10 %) than in the reference period (1991–2020). The exception is summer, for which a general decrease is expected, by more than 20 % in the case of GWL4.

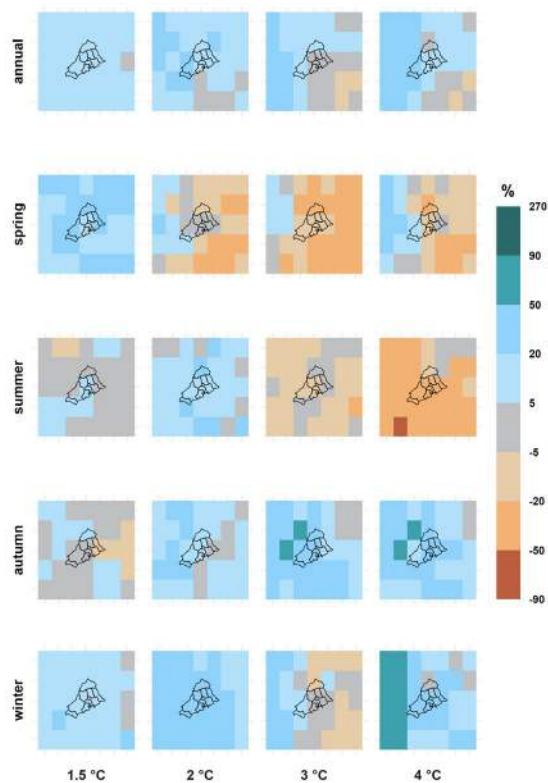
The annual maximum values of 1- to 5-day precipitation will be higher in the future, by between 5 and 10 %, mainly due to increases in winter (up to 10 %), as a decreasing trend with increasing GWL is observed for all multi-day extremes in summer (**FIGURE 11**). The extremes will be stronger and more frequent in the future, as the number of days above the 97th percentile on an annual level will also increase by around 20 % relative to the reference period (25 % for 1-day precipitation and 20 % for 2- and 3-day precipitation). The seasonal increase in frequency is greatest in winter, by around 40 % for 1-day precipitation and by around 30 % for 2- and 3-day precipitation. The expected increase is lowest in spring and summer (less than 20 % relative to the reference period).

FIGURE 11: Relative changes in the intensity (top) and frequency (bottom) of 3-day extreme precipitation events for four global warming levels relative to 1991–2020, represented by the median of the model simulation ensemble.



Rx3d

NUMBER OF DAYS ABOVE THE 97TH PERCENTILE FOR 3-DAY PRECIPITATION



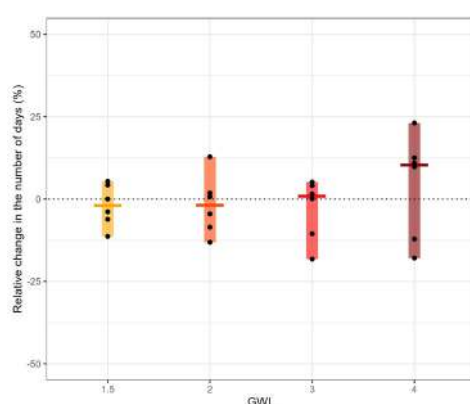
R97pN_3d

HOW WILL EXTREME WIND SPEED EVENTS CHANGE?

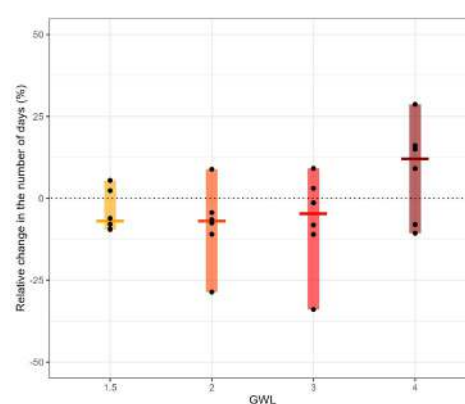
The frequency of days on which the daily mean wind speed exceeds the 97th percentile of the reference period shows a slight increase of about 10 % on an annual level and for winter under GWL4 (**FIGURE 12**), but these changes are accompanied by a large uncertainty. For other seasons and global warming levels, the changes are even smaller, with some even showing a decrease in the number of events.

The annual and seasonal maxima of the daily mean wind speed also show a small increase under GWL4 (**FIGURE 13**), particularly for winter, where the maximum daily mean wind speed is expected to increase by approximately 3 % (0.3 m/s), but both changes on an annual level and for winter are accompanied by large uncertainties.

NUMBER OF DAYS ABOVE THE 97TH PERCENTILE FOR DAILY MEAN WIND SPEED, ANNUAL



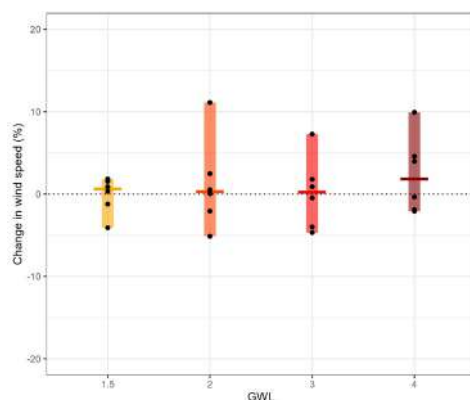
NUMBER OF DAYS ABOVE THE 97TH PERCENTILE FOR DAILY MEAN WIND SPEED, WINTER



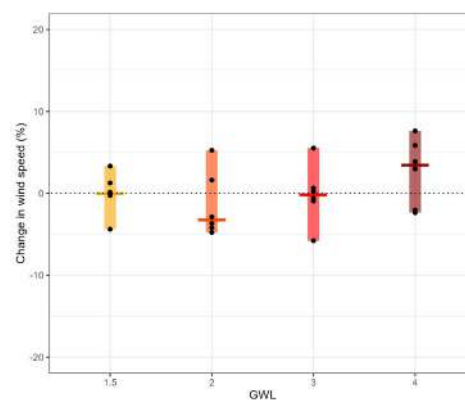
WS97pN_1d*

FIGURE 12: Relative change in the number of days on which the daily mean wind speed exceeds the 97th percentile of the reference period on an annual level (left) and for winter (right) for four global warming levels relative to 1991–2020, averaged over the wider area of the Arly river catchment. The bars show the range and median of the model simulation ensemble.

MAX. DAILY MEAN WIND SPEED, ANNUAL



MAX. DAILY MEAN WIND SPEED, WINTER



WSx1d*

FIGURE 13: Relative change in maximum daily mean wind speed on an annual level (left) and for winter (right) for four global warming levels relative to 1991–2020, averaged over the wider area of the Arly river catchment. The bars show the range and median of the model simulation ensemble.

METHODOLOGY



ASSESSMENT OF TRENDS AND PROBABILITY OF OCCURRENCE

Trends, except trends in extreme values, were assessed with Theil-Sen estimator. The frequency of extreme values was estimated with classical extreme value theory (fitting corresponding data to the generalised extreme value distribution), and trends in extreme values with non-stationary extreme value theory. The collective significance of the trends on a given pilot area (field significance) was evaluated from individual significance tests, controlling the false discovery rate. The methodology of each method is briefly described below.

Trend assessment with Theil-Sen estimator

Trends for values not connected to extreme values were estimated with Theil-Sen estimator or Sen's slope estimator. This is a robust method of linear regression that is not influenced by outliers. It is nonparametric method and does not assume any specific distribution for the data. On the other hand, it is hardly less reliable in the cases where all conditions for the least square method are met. Calculation of trends is quite simple: it is the median of all possible slopes formed by pairs of points for a given collection of data points. Each pair contributes to the slope calculation, regardless of whether the points lie on a straight line or not. At the same time an accurate confidence interval for the trend can be estimated even when there are nonnormality and heteroscedasticity (Wilcks, 2016).

Statistical significance of the time series was assessed with Mann-Kendall trend test. It is a nonparametric test, without assuming normality, but the data should have no serial correlation. The null hypothesis was rejected when the p-value associated with Mann-Kendall statistics was lower than 0.05 or 0.10 respectively. Non-serial correlation, if existed, was achieved by Zhang's method of pre-whitening (Wang and Swail, 2001).

Generalized extreme value distribution (GEV) and estimation of return periods of extreme events

The probability of extreme events was calculated with classical extreme value theory. The classical extreme value theory focuses on the statistical behaviour of extreme values of block maxima, usually corresponding to the annual or seasonal maxima. If the process is stationary, then under quite common conditions, for some large value of blocks (which in our case corresponds to the number of years) block maxima have a limiting distribution, called *generalised extreme value distribution* (GEV distribution) (Coles, 2001). The GEV distribution is a family of continuous probability distributions with three parameters: location (μ), scale (σ) and shape parameter (ξ).

Block maxima are fit to GEV distribution with maximum likelihood estimation, which also makes possible the estimation of confidence intervals for parameters and return levels.

Estimates of extreme quantiles of the annual maximum distribution were obtained from the GEV distribution and expressed in the form of return levels z_p . The return level z_p is associated with the return period $1/p$, where p is the probability of occurrence for the value z_p or more. More precisely, z_p is exceeded by the annual maximum in any particular year with probability p (Coles, 2001).

If a large number of years considered had study quantity equal to zero, the probability for the selected event was adjusted. This adjustment was made by dividing the probability by the ratio of years with non-zero data and total number of years for which data were available.

Trend assessment for extreme values

The GEV distribution is valid for block extremes for stationary sequence. It can be generalised to non-stationary

processes, e.g. for those with trends, possibly due to long-term climate changes. This can be achieved with GEV distribution with time dependent parameters; in our case appropriate model was linear in location parameter only:

$$\mu(t) = \mu_0 + \mu_1 t$$

The parameter μ_1 corresponds to the annual rate of change in annual maximum value of the variable it concerns. For linear model that means that the levels with all return periods change for the same amount in time. More complex models were also examined but they were mostly statistically insignificant. Statistical significance of the models is checked with the *likelihood ratio test* (Coles, 2001).

Field significance

The collective significance of the trends (field significance) was evaluated from individual significance tests. The straightforward approach, *controlling the false discovery rate* (FDR), was chosen to protect against overstatement or overinterpretation of multiple-testing results (Wilks, 2016). The idea of the method is to construct the meta-test which uses the results of many individual tests to address the global null hypothesis that all individual local (i.e., in grid points or in measurement points) null hypothesis are true. If the global null hypothesis cannot be rejected, it cannot be concluded with confidence that any of the individual local tests show meaningful violation of their respective null hypotheses. The failure to achieve field significance protects us to a degree from being misled into believing results from many erroneous rejections of true local null hypothesis that will invariably occur. We have chosen $\alpha_{FDR} = 2\alpha_{global}$ which produces approximately correct global test levels for data grids exhibiting moderate to strong spatial correlations (Wilks, 2016).

ANALYSIS OF PROJECTED CHANGES UNDER DIFFERENT GLOBAL WARMING LEVELS

The projected changes in the pilot area were assessed for different levels of global warming by considering the available EURO-CORDEX projections listed under Data. The global warming levels (GWLs) considered were +

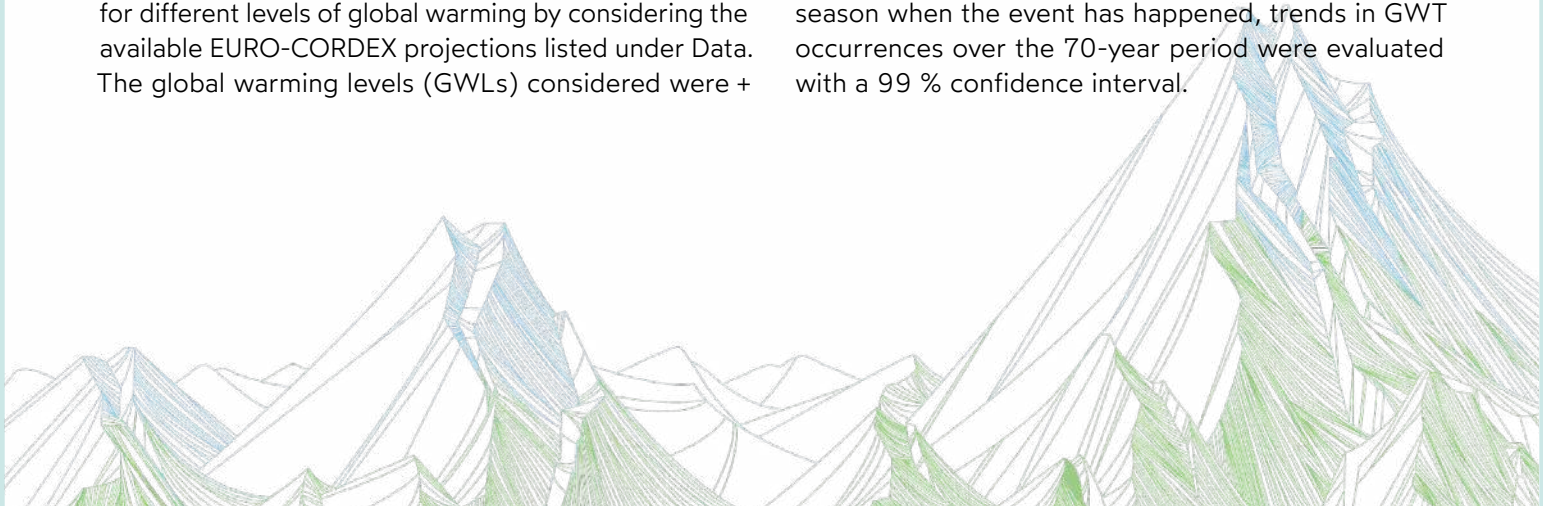
1.5, + 2, + 3 and + 4 °C with respect to the pre-industrial baseline period 1850-1900, following the approach included in the Sixth Assessment Report of the Intergovernmental Panel on Climate Change (IPCC, 2021). For each GWL, the corresponding 20-year period when global mean temperature reaches that level of increase with respect to the baseline period was identified for each model and RCP (Representative Concentration Pathway) simulation (https://github.com/mathause/cmip_warming_levels). Since some models and RCP scenarios do not include all GWLs, only simulations covering all considered GWLs were considered, namely RCP 8.5 simulations.

It is important to note, that GWLs cannot be translated into a specific temporal interval since it varies among the models. However, for assigning a temporal horizon to projected results, the highest GWL3 and GWL4 are reached by models in the second half of the 21st century under high emission scenarios.

For the assessment of future changes and return periods, the 20-year interval associated with each GWL was considered and extended over a 30-year period by adding 5 years before and after the GWL interval. Projected changes were evaluated for selected model simulations relative to the 1991–2020 baseline and reported as model ensemble median and range.

ANALYSIS OF SYNOPTIC CONDITIONS FOR PILOT EVENTS

Mean sea level pressure (MSLP) data from -80° West to 40° East and 30° to 70° North for the last 70 years from the ERA5 reanalysis was used to calculate 'Gross-Wetter-Typen' (GWT), which is a circulation type classification and is based on correlations between mean sea level pressure fields that are grouped into 18 clusters. The COST733 (Philip et al., 2014) software was used for that. Specific pilot events were then characterised by the mean GWT pattern derived over 7 decades of ERA5 data and by analysing the specific daily MSLP pattern at event occurrence. Furthermore, for the specific season when the event has happened, trends in GWT occurrences over the 70-year period were evaluated with a 99 % confidence interval.



REFERENCES



Barthelon, C., 2018. Retour d'expérience sur les événements de janvier 2018 dans les Alpes du Nord: Les particularités de cette crise. *Séminaire transversal Science-Décision-Action "La gestion des nombreux incidents de janvier 2018: cas isolé ou scénario de dimensionnement pour les années futures?"* Chambéry, 16th October 2018.

Coles, S., 2001. An Introduction to Statistical Modeling of Extreme Values. Springer, London, 209 pp.

Drias, data Météo-France, CERFACS, IPSL, 2024. DRIAS Les futurs du climat. URL: <https://drias-prod.meteo.fr/> (Accessed 22nd February 2024)

IPCC, 2021. Climate Change 2021: The Physical Science Basis. Contribution of Working Group I to the Sixth Assessment Report of the Intergovernmental Panel on Climate Change [Masson-Delmotte, V., P. Zhai, A. Pirani, S.L. Connors, C. Péan, S. Berger, N. Caud, Y. Chen, L. Goldfarb, M.I. Gomis, M. Huang, K. Leitzell, E. Lonnoy, J.B.R. Matthews, T.K. Maycock, T. Waterfield, O. Yelekçi, R. Yu, and B. Zhou (eds.)]. Cambridge University Press, Cambridge, United Kingdom and New York, NY, USA, In press, doi: [10.1017/9781009157896](https://doi.org/10.1017/9781009157896)

IRMa, 2018. L'hiver le plus long. *Risques Infos* n°37, September 2018.

Lescurier, A. 2018. REX événements nivo-météo du 29 décembre au 8 janvier 2018. *Séminaire transversal Science-Décision-Action "La gestion des nombreux incidents de janvier 2018: cas isolé ou scénario de dimensionnement pour les années futures?"*, Chambéry, 16th October 2018.

PARN, 2018. La gestion des nombreux incidents de janvier 2018: cas isolé ou scénario de dimensionnement pour les années futures? *Séminaire transversal Science-Décision-Action*,

Chambéry, 16th October 2018. URL: <https://risknat.org/seminaire-transversal-sda-gestion-des-incidents-de-janvier-2018-risques-naturels-alpes-changement-climatique/>

Philipp, A., Beck, C., Esteban, P., Kreienkamp, F., Krennert, T., Lykoudis, S.P., Pianko-Kluczynska, K., Post, P., Rasilla-Alvarez, D., Spekat, A., Streicher, F., 2014. *COST733CLASS v1.2 User guide*.

Scherrer, S. C., Fischer, E. M., Posselt, R., Liniger, M. A., Croci-Maspoli, M., Knutti, R., 2016. Emerging trends in heavy precipitation and hot temperature extremes in Switzerland. *J. Geophys. Res. Atmos.*, 121, 2626-2637, doi: [10.1002/2015JD024634](https://doi.org/10.1002/2015JD024634)

Stoffel, M., Corona, C. 2018. Future winters glimpsed in the Alps. *Nature Geoscience*, 11(7), 458–460, doi: [10.1038/s41561-018-0177-6](https://doi.org/10.1038/s41561-018-0177-6)

Vautard, R., van Oldenborgh, G. J., Otto, F. E. L., Yiou, P., de Vries, H., van Meijgaard, E., et al., 2019. Human influence on European winter wind storms such as those of January 2018. *Earth System Dynamics*, 10(2), 271-286., doi: [10.5194/esd-2018-57](https://doi.org/10.5194/esd-2018-57)

Wang, X. L., and Swail, V. R., 2001. Changes of Extreme Wave Heights in Northern Hemisphere Oceans and Related Atmospheric Circulation Regimes. *J. Climate*, 14, 2204-2221, doi: [10.1175/1520-0442\(2001\)014<2204:COEWHI>2.0.CO;2](https://doi.org/10.1175/1520-0442(2001)014<2204:COEWHI>2.0.CO;2)

Wilcoxon, R. R., 2001. Fundamentals of Modern Statistical Methods. Springer, New York, 258 pp.

Wilks, D. S., 2016. The Stippling Shows Statistically Significant Grid Points: How Research Results are Routinely Overstated and Overinterpreted, and What to Do about It. *Bull. Amer. Meteor. Soc.*, 97, 2263–2273, doi: [10.1175/BAMS-D-15-00267.1](https://doi.org/10.1175/BAMS-D-15-00267.1)

